



# Promotional effect of Nb additive on the activity and hydrothermal stability for the selective catalytic reduction of NO<sub>x</sub> with NH<sub>3</sub> over CeZrO<sub>x</sub> catalyst



Shipeng Ding, Fudong Liu\*, Xiaoyan Shi, Hong He\*\*

State Key Joint Laboratory of Environment Simulation and Pollution Control, Research Center for Eco-Environmental Sciences, Chinese Academy of Sciences, 18 Shuangqing Road, Haidian District, Beijing 100085, PR China

## ARTICLE INFO

### Article history:

Received 23 April 2015

Received in revised form 21 June 2015

Accepted 26 June 2015

Available online 17 July 2015

### Keywords:

Selective catalytic reduction

Nitrogen oxides

Diesel engine exhaust

Hydrothermal stability

CeNbZrO<sub>x</sub> mixed oxide

## ABSTRACT

The promotional mechanism of Nb addition on the activity and hydrothermal stability of CeZr<sub>2</sub>O<sub>x</sub> catalyst for the selective catalytic reduction of NO<sub>x</sub> with NH<sub>3</sub> (NH<sub>3</sub>-SCR) was investigated by various methods including N<sub>2</sub>-physisorption, XRD, H<sub>2</sub>-TPR and *in situ* DRIFTS. The Nb-promoted CeZr<sub>2</sub>O<sub>x</sub> catalyst showed remarkable NH<sub>3</sub>-SCR activity together with excellent N<sub>2</sub> selectivity, SO<sub>2</sub>/H<sub>2</sub>O resistance and outstanding hydrothermal stability. The characterization results showed that the introduction of Nb to CeZr<sub>2</sub>O<sub>x</sub> not only resulted in the high surface area and strong redox ability, but also promoted the adsorption and activation of NH<sub>3</sub> and enhanced the reactivity of adsorbed nitrate together with NH<sub>3</sub> species. All the above features were favorable for the superior NH<sub>3</sub>-SCR performance. In addition, the CeNb<sub>3.0</sub>Zr<sub>2</sub>O<sub>x</sub> catalysts hydrothermally aged below 800 °C still possessed high redox ability and abundant acid sites, all of which were responsible for the excellent hydrothermal durability. The novel CeNb<sub>3.0</sub>Zr<sub>2</sub>O<sub>x</sub> catalyst was a promising candidate for the removal of NO<sub>x</sub> from diesel engine.

© 2015 Elsevier B.V. All rights reserved.

## 1. Introduction

Nitrogen oxides (NO<sub>x</sub>), emitted from mobile resources such as diesel engines and stationary resources like coal-fired power plants have been major atmospheric pollutants. The selective catalytic reduction of NO<sub>x</sub> with NH<sub>3</sub> (NH<sub>3</sub>-SCR) is the most widely employed technique to control the emission of NO<sub>x</sub>, and the most commercially used catalyst is V<sub>2</sub>O<sub>5</sub>-WO<sub>3</sub>/TiO<sub>2</sub> [1–3]. However, there still remains room for improvement with this catalyst system, such as low hydrothermal stability, a narrow operating temperature window and the unselective oxidation of NH<sub>3</sub> which produces ozone-depleting N<sub>2</sub>O at high temperatures [2,4,5]. Consequently, it is of great significance to develop novel NH<sub>3</sub>-SCR catalysts, with outstanding low-temperature NO<sub>x</sub> conversion, high N<sub>2</sub> selectivity, excellent hydrothermal stability and a broad operating temperature window, which will substitute for the conventional V<sub>2</sub>O<sub>5</sub>-WO<sub>3</sub>/TiO<sub>2</sub> catalyst.

CeO<sub>2</sub> was used as oxygen storage component of conventional three-way catalysts (TWCs) in the late 1980s [6]. However, pure CeO<sub>2</sub> showed poor stability and was susceptible sintering at high temperatures. The introduction of ZrO<sub>2</sub> to CeO<sub>2</sub> resulted in effectively improving the thermal stability of CeO<sub>2</sub> [6,7]. In model Pd three-way catalysts, catalysts prepared on the CeZrO<sub>x</sub> solid solution retained larger oxygen storage capacity than those based on pure CeO<sub>2</sub> after aging [7]. The CeZrO<sub>x</sub> is considered to be one of the most promising materials for NO<sub>x</sub> removal [8]. It was reported that the WO<sub>3</sub>/CeO<sub>2</sub>-ZrO<sub>2</sub> catalyst exhibited nearly 100% NO<sub>x</sub> conversion in the temperature range of 200–500 °C, and also showed higher thermal stability in comparison to the conventional V<sub>2</sub>O<sub>5</sub>-WO<sub>3</sub>/TiO<sub>2</sub> catalyst in NH<sub>3</sub>-SCR reaction [9]. Gao et al. developed a novel Ce catalyst supported on sulfated ZrO<sub>2</sub> for NH<sub>3</sub>-SCR reaction, which showed superior catalytic activity due to the well dispersion of CeO<sub>2</sub>, abundant acid sites together with increasing surface area and enrichment of Ce<sup>3+</sup> after sulfation [10]. Ce<sub>0.75</sub>Zr<sub>0.25</sub>O<sub>2</sub>-PO<sub>4</sub><sup>3-</sup> catalyst prepared by impregnating phosphates on Ce<sub>0.75</sub>Zr<sub>0.25</sub>O<sub>2</sub> still presented high SCR activity at 300–400 °C after hydrothermal-aged at 760 °C for 48 h, which might result from the fact that phosphates improved NH<sub>3</sub> adsorption and suppressed the unselective oxidation of NH<sub>3</sub> at high temperatures [11]. It was also found that the morphology of CeZrO<sub>x</sub> had a significant influence on the performance of MnO<sub>x</sub>/CeO<sub>2</sub>-ZrO<sub>2</sub> catalyst for the NH<sub>3</sub>-SCR

\* Corresponding author. Present address: Materials Sciences Division, Lawrence Berkeley National Laboratory, 1 Cyclotron Road, Berkeley, CA 94720, United States.

\*\* Corresponding author. Fax: +86 10 62849123.

E-mail addresses: [fudongliu@lbl.gov](mailto:fudongliu@lbl.gov), [lfid1982@gmail.com](mailto:lfid1982@gmail.com) (F. Liu), [honghe@rcees.ac.cn](mailto:honghe@rcees.ac.cn) (H. He).

reaction, and MnO<sub>x</sub>/CeO<sub>2</sub>-ZrO<sub>2</sub> nanorods exhibited higher activity than nanotubes and nanopolyhedra [12]. MnO<sub>x</sub>/Ce<sub>0.9</sub>Zr<sub>0.1</sub>O<sub>2</sub> nanorods exhibited better NO<sub>x</sub> reduction activity than Ce<sub>0.9</sub>Zr<sub>0.1</sub>O<sub>2</sub>. At the same time, experimental results together with density functional theory calculations clearly demonstrated that MnO<sub>x</sub> species could easily form an oxygen vacancy distortion and were highly dispersed on the surface of Ce<sub>0.9</sub>Zr<sub>0.1</sub>O<sub>2</sub> nanorods [13].

In addition, Nb-containing compounds and materials are currently essential catalysts for a variety of reactions, like the hydrogenation of alkane and the catalytic removal of nitrogen oxides [14]. It was reported that the NH<sub>3</sub>-SCR reactivity of Nb-containing MnO<sub>x</sub>-CeO<sub>2</sub> was dramatically improved as a result of Nb addition, and the characterization results indicated that the strong interaction between Nb and Mn catalytic active sites resulted in a remarkable dispersion of the oxidizing sites together with acidic sites and inhibited the unselective NH<sub>3</sub> oxidation at high temperatures [15]. CeO<sub>2</sub>-Nb<sub>2</sub>O<sub>5</sub> catalyst containing abundant surface adsorbed oxygen, which might result from the short-range activation effect of Nb to Ce species, also exhibited excellent SCR performance [16].

Therefore, in the present work, a series of Nb-promoted CeZr<sub>2</sub>O<sub>x</sub> catalysts was prepared by a homogeneous precipitation method and was applied in the NH<sub>3</sub>-SCR process. The obtained CeNb<sub>3.0</sub>Zr<sub>2.0</sub>O<sub>x</sub> catalyst exhibited excellent SCR activity, N<sub>2</sub> selectivity, SO<sub>2</sub>/H<sub>2</sub>O resistance and hydrothermal durability. The structure, redox ability and reactivity of adsorbed NO<sub>x</sub> and NH<sub>3</sub> species on the catalysts were systematically characterized using various methods including N<sub>2</sub> physisorption, XRD, H<sub>2</sub>-TPR and *in situ* DRIFTS. The characterization results indicated that the addition of Nb significantly improved the surface area, redox ability and reactivity of adsorbed nitrate together with NH<sub>3</sub> species. High redox ability and abundant acid sites still existed on CeNb<sub>3.0</sub>Zr<sub>2.0</sub>O<sub>x</sub> catalysts hydrothermally aged below 800 °C.

## 2. Experimental

### 2.1. Catalysts preparation and activity test

A homogeneous precipitation method using urea as precipitant was applied to prepare the pure Nb<sub>2</sub>O<sub>5</sub> and CeNb<sub>a</sub>Zr<sub>2</sub>O<sub>x</sub> catalysts. In a typical preparation process, the desired amount of Ce(NO<sub>3</sub>)<sub>3</sub>·6H<sub>2</sub>O, NbCl<sub>5</sub> and Zr(NO<sub>3</sub>)<sub>4</sub>·5H<sub>2</sub>O were dissolved in deionized water, respectively. Superfluous urea was then added into the mix solution, with continuous stirring at 90 °C for 12 h. Subsequently, the precipitate was collected by filtration and washing with excess deionized water, dried at 100 °C overnight and calcined at 500 °C for 3 h. The catalysts were denoted as CeNb<sub>a</sub>Zr<sub>2</sub>O<sub>x</sub> (a = 0, 0.5, 1.0, 3.0, 6.0) where a represented the molar ratio of Nb/Ce, and the Ce/Zr molar ratio was fixed at 1:2. The expected weight percentages of components in CeNb<sub>a</sub>Zr<sub>2</sub>O<sub>x</sub> catalysts are shown in Table S1 in Supporting information. For comparison, commercial V<sub>2</sub>O<sub>5</sub>-WO<sub>3</sub>/TiO<sub>2</sub> catalyst with 2 wt.% V<sub>2</sub>O<sub>5</sub> and 10 wt.% WO<sub>3</sub> was also prepared using the conventional impregnation method. All the catalysts were crushed and sieved to 40–60 mesh for activity evaluation.

The hydrothermal-aged CeNb<sub>3.0</sub>Zr<sub>2.0</sub>O<sub>x</sub> catalysts were also obtained by treating the fresh samples in air containing 10 vol.% H<sub>2</sub>O at desired temperature for 8 h or 48 h with a GHSV of 10,000 h<sup>-1</sup>. The hydrothermal-aged samples were denoted as CeNb<sub>3.0</sub>Zr<sub>2.0</sub>O<sub>x</sub>-t, where t represented the treatment temperature in °C.

The NH<sub>3</sub>-SCR activity of samples was performed in a fixed-bed quartz tube reactor at atmospheric pressure. The experimental conditions were as follows: 500 ppm NO, 500 ppm NH<sub>3</sub>, 5 vol.% O<sub>2</sub>, 100 ppm SO<sub>2</sub> (when used), 5 vol.% H<sub>2</sub>O (when used), N<sub>2</sub> balance and flow rate of 500 mL/min. The effluent gas was continuously

analyzed by an FTIR spectrometer (Nicolet Nexus 670) which was equipped with a heated, low volume multiple-path gas cell (2 m). The FTIR spectra were collected after 1 h while the NH<sub>3</sub>-SCR reaction reached a steady state. NO<sub>x</sub> conversion and N<sub>2</sub> selectivity were calculated as follows:

$$\text{NO}_x \text{ conversion} = \left(1 - \frac{[\text{NO}]_{\text{out}} + [\text{NO}_2]_{\text{out}}}{[\text{NO}]_{\text{in}} + [\text{NO}_2]_{\text{in}}}\right) \times 100\%$$

$$\text{N}_2 \text{ selectivity} = \frac{[\text{NO}]_{\text{in}} + [\text{NH}_3]_{\text{in}} - [\text{NH}_2]_{\text{out}} - 2[\text{N}_2\text{O}]_{\text{out}}}{[\text{NO}]_{\text{in}} + [\text{NH}_3]_{\text{in}}} \times 100\%$$

### 2.2. Characterization

The N<sub>2</sub> adsorption-desorption isotherms over Nb<sub>2</sub>O<sub>5</sub>, CeNb<sub>a</sub>Zr<sub>2</sub>O<sub>x</sub> and hydrothermal-aged CeNb<sub>3.0</sub>Zr<sub>2.0</sub>O<sub>x</sub> catalysts were achieved using a Quantachrome Autosorb-1C instrument at liquid N<sub>2</sub> temperature (77 K). Before the N<sub>2</sub> physisorption, all the catalysts were outgassed at 300 °C for 5 h in vacuum. The specific surface areas were calculated by BET equation at P/P<sub>0</sub> in the partial pressure range of 0.05–0.35.

Powder X-ray diffraction (XRD) patterns of the samples were conducted on a computerized PANalytical X'Pert Pro diffractometer with Cu Kα (λ = 0.15406 nm) radiation. The data of 2θ from 20 to 80° were collected at a step of 8°/min with the step size of 0.07°.

The H<sub>2</sub>-TPR experiments were carried out on a Micromeritics AutoChem 2920 chemisorption analyzer. In a typical measurement, 100 mg of the sample was firstly preprocessed in a flow of 20 vol.% O<sub>2</sub>/N<sub>2</sub> with the total flow rate of 50 mL/min at 400 °C for 0.5 h, and then lowered the temperature to ambient temperature (30 °C) followed by Ar purging for another 0.5 h. Then the temperature was linearly increased from 30 to 1000 °C at the heating rate of 10 °C/min in a flow of 10 vol.% H<sub>2</sub>/Ar (50 mL/min). The H<sub>2</sub> consumption amount was detected by a thermal conductivity detector (TCD).

The *in situ* DRIFTS experiments were performed on an FTIR spectrometer (Nicolet Nexus 670) equipped with a smart collector and an MCT/A detector, which was cooled by liquid nitrogen. Prior to each experiment, the catalyst was pretreated in 20 vol.% O<sub>2</sub>/N<sub>2</sub> at 400 °C for 0.5 h and then cooled down to 200 °C. The background spectrum which was collected in flowing N<sub>2</sub> was automatically subtracted from the sample spectrum. The reaction conditions were as follows: 500 ppm NH<sub>3</sub>, 500 ppm NO, 5 vol.% O<sub>2</sub>, N<sub>2</sub> balance and 300 mL/min total flow rate. All spectra were recorded by accumulating 100 scans with a resolution of 4 cm<sup>-1</sup>.

## 3. Results and discussion

### 3.1. NH<sub>3</sub>-SCR activity

The NO<sub>x</sub> conversion and N<sub>2</sub> selectivity in NH<sub>3</sub>-SCR reaction over pure Nb<sub>2</sub>O<sub>5</sub> and CeNb<sub>a</sub>Zr<sub>2</sub>O<sub>x</sub> catalysts with different Nb contents under a GHSV of 50,000 h<sup>-1</sup> are shown in Fig. 1. CeZr<sub>2</sub>O<sub>x</sub> exhibited low NO<sub>x</sub> conversion, poor N<sub>2</sub> selectivity along with a narrow operating temperature window, and the maximum NO<sub>x</sub> conversion was only 90% at 350 °C. Pure Nb<sub>2</sub>O<sub>5</sub> sample showed negligible SCR activity and the NO<sub>x</sub> conversion was below 10% in the whole temperature range. Nevertheless, for Nb-containing CeNb<sub>a</sub>Zr<sub>2</sub>O<sub>x</sub> catalysts, the addition of Nb resulted in a great enhancement of NO<sub>x</sub> conversion both in low and high temperatures, high N<sub>2</sub> selectivity and a broad temperature window, which indicated that the coexistence of Nb and CeZr<sub>2</sub>O<sub>x</sub> species was of essential importance for high NH<sub>3</sub>-SCR performance. CeNb<sub>3.0</sub>Zr<sub>2.0</sub>O<sub>x</sub> catalyst with the molar ratio of Nb:Ce = 3.0:1 showed the highest NH<sub>3</sub>-SCR performance in the entire temperature range, over which the complete removal of NO<sub>x</sub> was accomplished from 225 to 425 °C under the GHSV of 50,000 h<sup>-1</sup>. The NO<sub>x</sub> conversion was over 90% above 250 °C

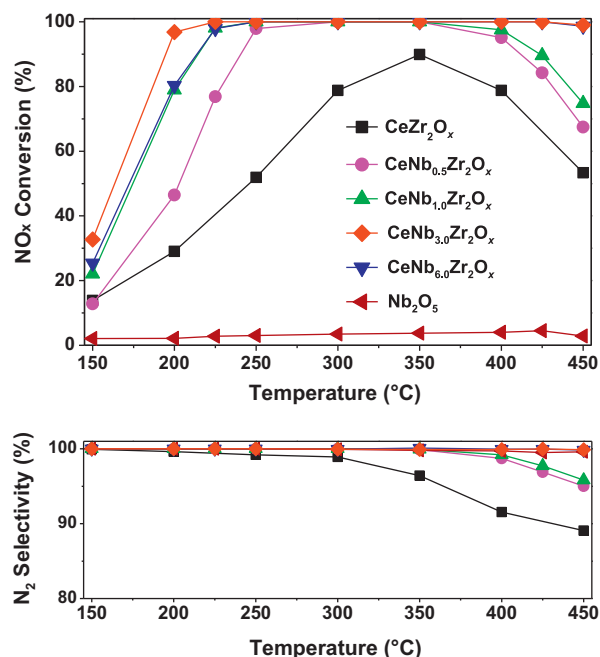


**Fig. 1.** NO<sub>x</sub> conversion and N<sub>2</sub> selectivity as a function of temperature over pure Nb<sub>2</sub>O<sub>5</sub> and CeNb<sub>a</sub>Zr<sub>2</sub>O<sub>x</sub> ( $a = 0, 0.5, 1.0, 3.0, 6.0$ ) catalysts in NH<sub>3</sub>-SCR reaction. Reaction conditions: [NO] = [NH<sub>3</sub>] = 500 ppm, [O<sub>2</sub>] = 5 vol.%, GHSV = 50,000 h<sup>-1</sup>.

even under a quite high GHSV of 200,000 h<sup>-1</sup> (see Fig. S1), which indicated that the obtained catalyst exhibited excellent resistance to high space velocity and was suitable to applications of diesel engines where there was only limited space for the installation of SCR catalysts. For conventional V<sub>2</sub>O<sub>5</sub>-WO<sub>3</sub>/TiO<sub>2</sub> catalyst, one of the inevitable drawbacks was the unselective oxidation of NH<sub>3</sub> at high temperatures, which would lower the NO<sub>x</sub> conversion and produce a large amount of N<sub>2</sub>O. However, the N<sub>2</sub> selectivity of novel CeNb<sub>3.0</sub>Zr<sub>2</sub>O<sub>x</sub> catalyst was as high as over 99% even at 450 °C, which was promising for the elimination of NO<sub>x</sub> from diesel engine exhaust. Further increasing the molar ratio of Nb/Ce from 3.0:1 to 6.0:1 would lead to a slight decrease of NO<sub>x</sub> conversion at low temperature, probably due to the coverage of active cerium sites by excess Nb species. In addition, the NH<sub>3</sub> conversion in NH<sub>3</sub>-SCR reaction over CeZr<sub>2</sub>O<sub>x</sub> and CeNb<sub>3.0</sub>Zr<sub>2</sub>O<sub>x</sub> is presented in Fig. S2. The results indicated that the introduction of Nb greatly improved the conversion of NH<sub>3</sub> at low temperatures, and the NH<sub>3</sub> was almost completely consumed over CeZr<sub>2</sub>O<sub>x</sub> and CeNb<sub>3.0</sub>Zr<sub>2</sub>O<sub>x</sub> samples at high temperatures. The NH<sub>3</sub>-SCR results indicated that some synergistic effect possibly exist between Nb, Ce and Zr species, which will be discussed later in this work.

### 3.2. Effect of H<sub>2</sub>O and SO<sub>2</sub>

In practical applications, the combustion exhaust containing water vapor and SO<sub>2</sub> may lead to the deactivation of NH<sub>3</sub>-SCR catalyst. Therefore, it was worthwhile to investigate the influence of H<sub>2</sub>O/SO<sub>2</sub> on the activity over CeNb<sub>3.0</sub>Zr<sub>2</sub>O<sub>x</sub> catalyst. As shown in Fig. 2(A), the addition of 5 vol.% H<sub>2</sub>O had a negligible inhibition effect on the NH<sub>3</sub>-SCR performance of CeNb<sub>3.0</sub>Zr<sub>2</sub>O<sub>x</sub> and the NO<sub>x</sub> conversion was almost 100% for the entire 24 h, suggesting that CeNb<sub>3.0</sub>Zr<sub>2</sub>O<sub>x</sub> catalyst exhibited strong resistance to H<sub>2</sub>O poisoning at 250 °C. The effect of 100 ppm SO<sub>2</sub> on CeNb<sub>3.0</sub>Zr<sub>2</sub>O<sub>x</sub> catalyst activity is shown in Fig. 2(B). The NO<sub>x</sub> conversion did not show any decrease for the first 14 h when SO<sub>2</sub> was introduced into the reaction atmosphere. However, further increasing the reaction time resulted in a slight decline and reduced to 80%, due to the deposition of ammonium sulfate/bisulfate on the surface, which might

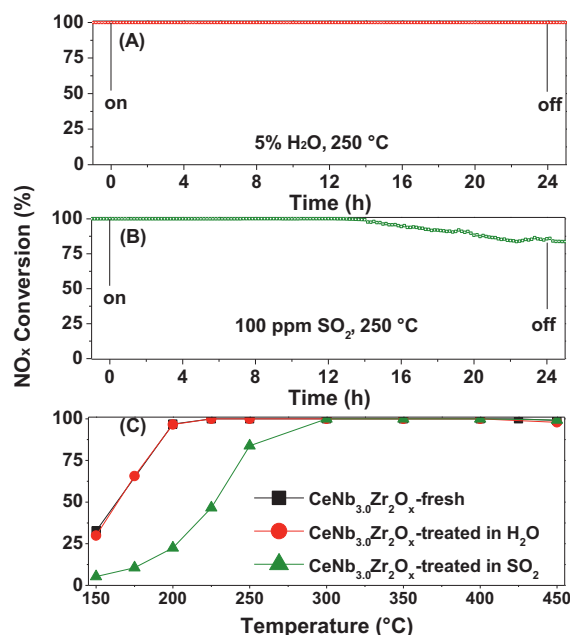


**Fig. 2.** The effect of H<sub>2</sub>O (A), SO<sub>2</sub> (B) on NH<sub>3</sub>-SCR activity over CeNb<sub>3.0</sub>Zr<sub>2</sub>O<sub>x</sub> catalyst with 5 vol.% H<sub>2</sub>O or 100 ppm SO<sub>2</sub> at 250 °C; (C) NO<sub>x</sub> conversion in NH<sub>3</sub>-SCR reaction as a function of temperature without H<sub>2</sub>O and SO<sub>2</sub> over CeNb<sub>3.0</sub>Zr<sub>2</sub>O<sub>x</sub> catalysts after treatment in H<sub>2</sub>O/SO<sub>2</sub> for 24 h. Reaction conditions: [NO] = [NH<sub>3</sub>] = 500 ppm, [O<sub>2</sub>] = 5 vol.%, [SO<sub>2</sub>] = 100 ppm (when used), [H<sub>2</sub>O] = 5 vol.% (when used), GHSV = 50,000 h<sup>-1</sup>.

block the active sites. In order to further study the influence of H<sub>2</sub>O/SO<sub>2</sub> poisoning on the performance of the catalysts treated in the NH<sub>3</sub>-SCR reaction at 250 °C for 24 h, the activity of CeNb<sub>3.0</sub>Zr<sub>2</sub>O<sub>x</sub> samples in Fig. 2(A) and (B) was retested in the absence of H<sub>2</sub>O and SO<sub>2</sub> and the results are shown in Fig. 2(C). It was obvious that CeNb<sub>3.0</sub>Zr<sub>2</sub>O<sub>x</sub> after treatment in H<sub>2</sub>O showed high activity, and nearly 100% NO<sub>x</sub> conversion was obtained between 200 and 450 °C, which was almost the same as that of the fresh catalyst. Even though the SO<sub>2</sub> treatment had a negative effect on the activity of CeNb<sub>3.0</sub>Zr<sub>2</sub>O<sub>x</sub>, the NO<sub>x</sub> conversion was still more than 80% above 250 °C. In short summary, the CeNb<sub>3.0</sub>Zr<sub>2</sub>O<sub>x</sub> catalyst exhibited high resistance to H<sub>2</sub>O and SO<sub>2</sub> poisoning, especially when the temperature was more than 250 °C, and could be used to eliminate the NO<sub>x</sub> from diesel engine exhaust containing a handful of H<sub>2</sub>O and SO<sub>2</sub>.

### 3.3. Promotional effect of Nb addition on the SCR activity

#### 3.3.1. N<sub>2</sub> physisorption

Fig. S3 shows the N<sub>2</sub> adsorption-desorption isotherms of the catalysts. It could be observed that all the samples displayed type IV isotherms in the relative pressure ( $P/P_0$ ) range of 0.4–0.8 according to the IUPAC classification, which were typical for mesoporous materials (2–50 nm) [17]. In addition, the BET surface area and

**Table 1**  
BET surface area and pore volume of Nb<sub>2</sub>O<sub>5</sub> and CeNb<sub>a</sub>Zr<sub>2</sub>O<sub>x</sub> samples.

Catalysts	S <sub>BET</sub> <sup>a</sup> (m <sup>2</sup> /g)	Pore volume <sup>b</sup> (cm <sup>3</sup> /g)
Nb <sub>2</sub> O <sub>5</sub>	68.4	0.11
CeZr <sub>2</sub> O <sub>x</sub>	107.3	0.13
CeNb <sub>0.5</sub> Zr <sub>2</sub> O <sub>x</sub>	170.1	0.25
CeNb <sub>1.0</sub> Zr <sub>2</sub> O <sub>x</sub>	198.1	0.20
CeNb <sub>3.0</sub> Zr <sub>2</sub> O <sub>x</sub>	208.7	0.18
CeNb <sub>6.0</sub> Zr <sub>2</sub> O <sub>x</sub>	206.5	0.17

<sup>a</sup> BET surface area.

<sup>b</sup> Total pore volume.

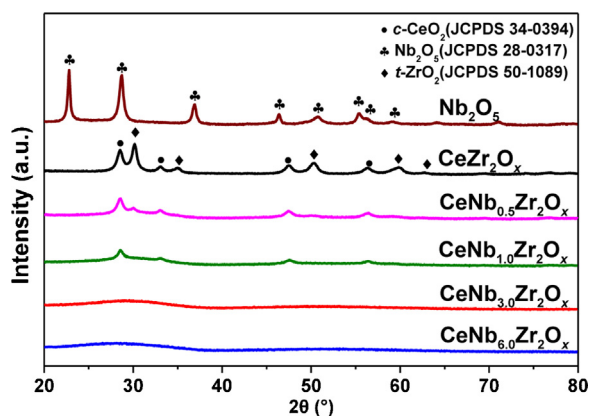


Fig. 3. Powder XRD of  $\text{Nb}_2\text{O}_5$  and  $\text{CeNb}_a\text{Zr}_2\text{O}_x$  catalysts with different Nb loadings.

pore volume derived from  $\text{N}_2$  physisorption results of  $\text{Nb}_2\text{O}_5$  and  $\text{CeNb}_a\text{Zr}_2\text{O}_x$  samples are shown in Table 1. It was obvious that the addition of  $\text{Nb}_2\text{O}_5$  to  $\text{CeZr}_2\text{O}_x$  had a great influence on the surface and pore volume of the samples. As the molar ratio of Nb/Ce increased from 0.5:1 to 3.0:1, the surface area of the corresponding samples grew significantly.  $\text{CeNb}_{3.0}\text{Zr}_2\text{O}_x$  catalyst, with molar ratio of Nb/Ce = 3.0:1, showed the largest surface area of  $208.7 \text{ m}^2/\text{g}$  among the Nb-containing catalysts, which was in consistent with the best  $\text{NH}_3$ -SCR performance. However, further improving the Nb/Ce molar ratio to 6.0:1 led to a slight decrease of the surface area. It was believed that, compared to  $\text{CeNb}_{3.0}\text{Zr}_2\text{O}_x$  catalyst,  $\text{CeNb}_{6.0}\text{Zr}_2\text{O}_x$  catalyst showed a slight decrease of  $\text{NO}_x$  conversion at low temperature, which possibly result from the coverage of active cerium sites by excess Nb species rather than the decline of surface area. These results indicated that the introduction of Nb could induce structural modification of the samples and lead to a higher surface area, which was beneficial for the dispersion of active components and resulted in high  $\text{NO}_x$  conversion over Nb-containing catalysts for  $\text{NH}_3$ -SCR [18].

### 3.3.2. XRD results

Powder XRD was conducted to investigate the crystal structural of  $\text{Nb}_2\text{O}_5$  and  $\text{CeNb}_a\text{Zr}_2\text{O}_x$  catalysts, and the results are shown in Fig. 3. The  $\text{CeZr}_2\text{O}_x$  catalyst provided typical diffraction patterns for the  $\text{ZrO}_2$  tetragonal phase (JCPDS 50-1089) and the  $\text{CeO}_2$  cubic phase (JCPDS 34-0394), which indicated that no strong interaction existed between Ce and Zr, leading to the segregation of  $\text{CeO}_2$  and  $\text{ZrO}_2$  crystallites [19]. With the improvement of Nb/Ce molar ratio, the band intensity ascribed to  $\text{CeO}_2$  and  $\text{ZrO}_2$  over Nb-containing catalysts decreased significantly. No diffraction peaks attributed to Nb species were detected in the XRD patterns for all the Nb-containing catalysts, indicating that Nb species existed as amorphous. For  $\text{CeNb}_{3.0}\text{Zr}_2\text{O}_x$  and  $\text{CeNb}_{6.0}\text{Zr}_2\text{O}_x$  catalysts, no obvious peak attributed to  $\text{CeO}_2$  or  $\text{ZrO}_2$  was observed suggesting the formation of homogeneously dispersed crystallites or a complete amorphous structure. Amorphous structure usually possessed larger surface area than the crystallized one [20], which might be one of the essential reasons why the surface area of Nb-containing catalysts was higher than that of  $\text{CeZr}_2\text{O}_x$  catalyst.

### 3.3.3. $\text{H}_2$ -TPR

$\text{H}_2$ -TPR experiments were performed to investigate the redox ability of  $\text{Nb}_2\text{O}_5$ ,  $\text{CeZr}_2\text{O}_x$  and  $\text{CeNb}_{3.0}\text{Zr}_2\text{O}_x$  catalysts, and the results are shown in Fig. 4. For the  $\text{CeZr}_2\text{O}_x$  catalyst, the reduction peak at about  $510^\circ\text{C}$  was assigned to the reduction of surface  $\text{Ce}^{4+}$  to  $\text{Ce}^{3+}$ , and the peak at  $736^\circ\text{C}$  could be attributed to the reduction of bulk  $\text{CeO}_2$  [21–23]. In addition, the reduction peak of  $\text{Nb}_2\text{O}_5$  was about  $873^\circ\text{C}$ , which was responsible for reduction of bulk  $\text{Nb}_2\text{O}_5$  to

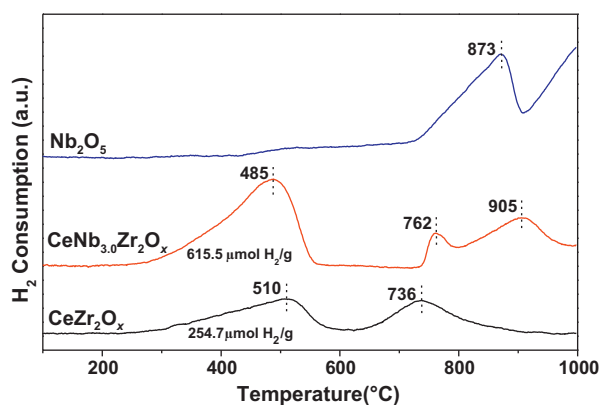


Fig. 4.  $\text{H}_2$ -TPR profiles of  $\text{Nb}_2\text{O}_5$ ,  $\text{CeZr}_2\text{O}_x$  and  $\text{CeNb}_{3.0}\text{Zr}_2\text{O}_x$  catalysts.

$\text{Nb}_2\text{O}_4$  [16,24]. Over  $\text{CeNb}_{3.0}\text{Zr}_2\text{O}_x$  catalyst, three reduction peaks centered at about  $485$ ,  $762$  and  $905^\circ\text{C}$  were observed. The two peaks at higher temperature belonged to the reduction of bulk  $\text{CeO}_2$  and  $\text{Nb}_2\text{O}_5$ , respectively. The reduction peak at  $485^\circ\text{C}$ , which was ascribed to the reduction of surface  $\text{Ce}^{4+}$  to  $\text{Ce}^{3+}$  showed lower reduction temperature in comparison to  $\text{CeZr}_2\text{O}_x$  sample, which indicated that redox ability of  $\text{CeNb}_{3.0}\text{Zr}_2\text{O}_x$  was greatly improved after the addition of Nb. Higher redox ability of  $\text{CeNb}_{3.0}\text{Zr}_2\text{O}_x$  could enhance the mobility of surface oxygen due to the strong synergistic effect among Zr, Ce and Nb species. It was believed that the synergistic effect led to severe structural distortion and affluent oxygen defects [25,26]. The oxygen defects promoted oxygen diffusion from the subsurface layers and might progressively proceed deeper into the bulk [27,28]. Furthermore, the  $\text{H}_2$  consumption for the reduction of surface  $\text{Ce}^{4+}$  to  $\text{Ce}^{3+}$  was calculated and the values are listed in Fig. 4. The results in Table S1 showed that the weight percentage of  $\text{CeO}_2$  in  $\text{CeNb}_{3.0}\text{Zr}_2\text{O}_x$  was lower than that in  $\text{CeZr}_2\text{O}_x$ . However, the  $\text{H}_2$  consumption of  $\text{CeNb}_{3.0}\text{Zr}_2\text{O}_x$  was  $615.5 \mu\text{mol H}_2/\text{g}_{\text{cat}}$ , which was higher than that of  $\text{CeZr}_2\text{O}_x$  ( $254.7 \mu\text{mol H}_2/\text{g}_{\text{cat}}$ ), indicating the formation of more reducible Ce species after the introduction of Nb to  $\text{CeZr}_2\text{O}_x$ . All the above features were beneficial for the excellent SCR activity.

### 3.3.4. $\text{NH}_3$ and $\text{NO}_x$ adsorption ability

The *in situ* DRIFTS of  $\text{NH}_3$  adsorption at  $200^\circ\text{C}$  was conducted to investigate the differences of acidity on the catalysts after Nb introduction and the results are illustrated in Fig. 5(A). After exposure to  $\text{NH}_3$  and  $\text{N}_2$  purge, the catalyst surface was mainly covered by a couple of  $\text{NH}_3$  species. The bands centered at  $1603 \text{ cm}^{-1}$  and  $1209$ ,  $1263$ ,  $1193$ ,  $1182 \text{ cm}^{-1}$  were assigned to asymmetric and symmetric bending vibrations of the N–H bonds in coordinated  $\text{NH}_3$  linked to Lewis acid sites, respectively [29–31]. In addition, the bands at  $3360$ ,  $3260$  and  $3155 \text{ cm}^{-1}$  were ascribed to N–H stretching modes of coordinated  $\text{NH}_3$  [32]. The bands at  $1668 \text{ cm}^{-1}$  and  $1434$ ,  $1444$ ,  $1414 \text{ cm}^{-1}$  attributed to symmetric and asymmetric bending vibrations of  $\text{NH}_4^+$  species on Brønsted acid sites were also observed [4,33–36]. Several negative bands around  $3700 \text{ cm}^{-1}$  ascribed to the hydroxyl consumption were also found, which might result from the reaction between hydroxyl and  $\text{NH}_3$  [4,25].

Pure  $\text{Nb}_2\text{O}_5$  showed slight amount of Brønsted acid sites and Lewis acid sites. However, the introduction of Nb to  $\text{CeZr}_2\text{O}_x$  resulted in more acid sites on the catalysts.  $\text{CeNb}_{3.0}\text{Zr}_2\text{O}_x$  catalyst, with Nb/Ce molar ratio of 3.0:1, exhibited the largest amount of  $\text{NH}_4^+$  bound to Brønsted acid sites and  $\text{NH}_3$  linked to Lewis acid sites among the series catalysts, which was quite in accordance with its highest  $\text{NH}_3$ -SCR performance. It has been reported that the surface acidity of  $\text{NbO}_x$ - $\text{MnO}_x$ - $\text{CeO}_2$  was significantly increased as a result of Nb addition [37]. In addition, the Nb–OH bond was

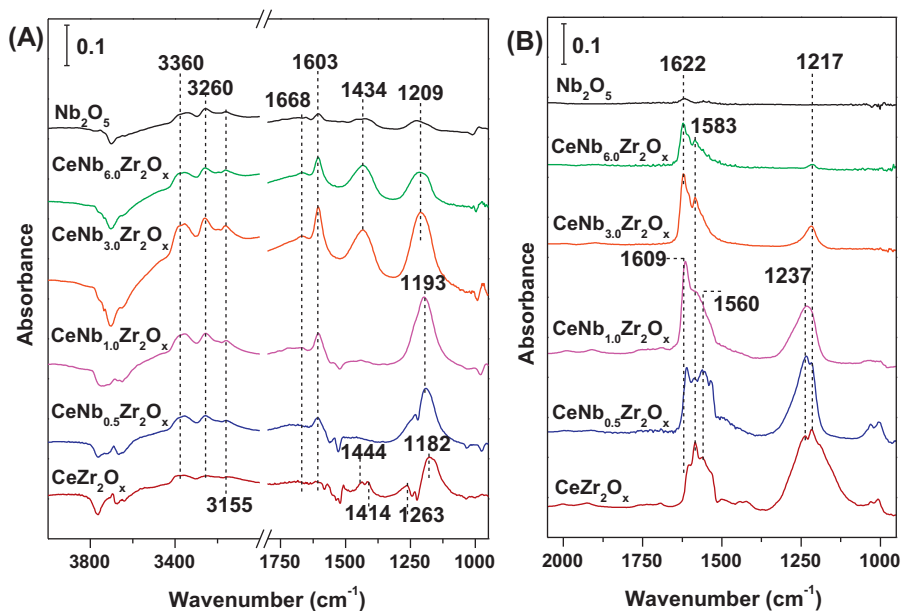


**Fig. 5.** *In situ* DRIFTS of 500 ppm  $\text{NH}_3$  adsorption (A) and 500 ppm  $\text{NO} + 5 \text{ vol.}\% \text{ O}_2$  adsorption (B) with 300 mL/min flow rate at  $200^\circ\text{C}$  on  $\text{Nb}_2\text{O}_5$  and  $\text{CeNb}_4\text{Zr}_2\text{O}_x$  series catalysts.

responsible for the Brønsted acid site and  $\text{Nb}=\text{O}$  bond for the Lewis acid site [16]. Further increasing the Nb/Ce molar ratio from 3.0 to 6.0 led to a slight decrease of acid sites. In addition, the desorption of adsorbed  $\text{NH}_3$  species at various temperatures over  $\text{CeZr}_2\text{O}_x$  and  $\text{CeNb}_{0.3}\text{Zr}_2\text{O}_x$  catalysts showed that  $\text{CeZr}_2\text{O}_x$  showed negligible amount of  $\text{NH}_3$  species at  $350^\circ\text{C}$ , while several bands still remained on  $\text{CeNb}_{3.0}\text{Zr}_2\text{O}_x$  sample (see Fig. S4). The results indicated that the introduction of Nb enhanced both the amount and strength of acid sites, which were beneficial for the adsorption together with activation of  $\text{NH}_3$ , leading to an excellent  $\text{NH}_3$ -SCR activity in the entire temperature range [14].

Fig. 5(B) shows the *in situ* DRIFTS results of  $\text{NO}_x$  adsorption over  $\text{Nb}_2\text{O}_5$  and  $\text{CeNb}_4\text{Zr}_2\text{O}_x$  catalysts. After  $\text{NO} + \text{O}_2$  adsorption for 1.0 h and  $\text{N}_2$  purge for another 0.5 h, a couple of distinct bands assigned to bidentate nitrate ( $1583$  and  $1560 \text{ cm}^{-1}$ ) and bridging nitrate ( $1609$ ,  $1622$ ,  $1237$  and  $1217 \text{ cm}^{-1}$ ) were observed [34,38–40]. It was quite clear that the introduction of Nb decreased both the intensity and quantity of bands assigned to nitrate species, which might arise from the fact that the addition of Nb promoted the formation of more acid sites together with fewer alkali sites where the nitrate species adsorbed [33]. It was also reported that the adsorption of nitrate species on  $\text{MnO}_x\text{-NbO}_x\text{-CeO}_2$  was weaker than that on  $\text{MnO}_x\text{-CeO}_2$  as a result of Nb addition [37].

### 3.3.5. Reactivity of adsorbed $\text{NH}_3$ species

The *in situ* DRIFTS reaction between pre-adsorbed  $\text{NH}_3$  and  $\text{NO} + \text{O}_2$  at  $200^\circ\text{C}$  was conducted to investigate the reactivity of adsorbed  $\text{NH}_3$  species. As shown in Fig. 6(A), the surface of  $\text{CeZr}_2\text{O}_x$  was mainly covered by ionic  $\text{NH}_4^+$  ( $1414$  and  $1444 \text{ cm}^{-1}$ ) and coordinated  $\text{NH}_3$  ( $3360$ ,  $3260$ ,  $1263$  and  $1160 \text{ cm}^{-1}$ ) after the catalyst was pre-adsorbed to  $\text{NH}_3$ . After the introduction of  $\text{NO} + \text{O}_2$ , the bands at  $1160 \text{ cm}^{-1}$  diminished in 5 min. However, the bands centered at  $1444$ ,  $1414$  and  $1263 \text{ cm}^{-1}$  were almost the same in 60 min, which might indicate that the adsorbed  $\text{NH}_3$  species over  $\text{CeZr}_2\text{O}_x$  were less active in the SCR reaction.

Compared to  $\text{CeZr}_2\text{O}_x$ , in Fig. 6(B), when  $\text{NO} + \text{O}_2$  was introduced to  $\text{CeNb}_{3.0}\text{Zr}_2\text{O}_x$  which was pre-exposed to  $\text{NH}_3$ , ionic  $\text{NH}_4^+$  ( $1668$  and  $1434 \text{ cm}^{-1}$ ) and coordinated  $\text{NH}_3$  ( $3360$ ,  $3260$ ,  $3155$ ,  $1603$

and  $1209 \text{ cm}^{-1}$ ) showed an apparent decrease in intensity due to the reaction between  $\text{NO} + \text{O}_2$  and  $\text{NH}_3$  species. After 3 min, all bands ascribed to  $\text{NH}_3$  species were replaced by nitrate species. The results indicated that both ionic  $\text{NH}_4^+$  and coordinated  $\text{NH}_3$  on  $\text{CeNb}_{3.0}\text{Zr}_2\text{O}_x$  were quite active in the SCR reaction. Therefore, it was safe to reach the conclusion that the introduction of Nb significantly improved the reaction activity of adsorbed  $\text{NH}_3$  species on  $\text{CeNb}_{3.0}\text{Zr}_2\text{O}_x$ .

### 3.3.6. Reactivity of adsorbed $\text{NO}_x$ species

The reactivity of adsorbed  $\text{NO}_x$  species in  $\text{NH}_3$ -SCR reaction on  $\text{CeZr}_2\text{O}_x$  and  $\text{CeNb}_{3.0}\text{Zr}_2\text{O}_x$  catalysts was also examined by the *in situ* DRIFTS of reaction between pre-adsorbed  $\text{NO}_x$  and  $\text{NH}_3$  at  $200^\circ\text{C}$ . For the  $\text{CeZr}_2\text{O}_x$  catalyst (Fig. 7(A)), after  $\text{NO} + \text{O}_2$  pre-adsorption and  $\text{N}_2$  purging, the catalyst surface was covered with bidentate nitrate ( $1583$  and  $1560 \text{ cm}^{-1}$ ) along with bridging nitrate ( $1609$ ,  $1217$  and  $1237 \text{ cm}^{-1}$ ). When  $\text{NH}_3$  was introduced, the intensity of the bands attributed to nitrate species did not show an obvious change. The adsorbed nitrate could not easily react with  $\text{NH}_3$  species. The results indicated that the adsorbed nitrate species over  $\text{CeZr}_2\text{O}_x$  catalyst were mostly inactive during the  $\text{NH}_3$ -SCR process.

As shown in Fig. 7(B), the surface of  $\text{CeNb}_{3.0}\text{Zr}_2\text{O}_x$  catalyst was mainly covered by bridging nitrate centered at  $1622$  and  $1217 \text{ cm}^{-1}$  and bidentate species around  $1583 \text{ cm}^{-1}$  after exposed to  $\text{NO} + \text{O}_2$ . When  $\text{NH}_3$  was introduced, the bands ascribed to bridging nitrate species were totally consumed in 3 min, however, the bidentate species did not decrease obviously which might indicate that the bridging nitrate rather than bidentate nitrate could react with  $\text{NH}_3$ . In addition, the bands corresponding to ionic  $\text{NH}_4^+$  and coordinated  $\text{NH}_3$  were appeared after 5 min. From the comparison between Fig. 7(A) and (B), it was believed that the adsorbed nitrate species on  $\text{CeNb}_{3.0}\text{Zr}_2\text{O}_x$  were more reactive than those on  $\text{CeZr}_2\text{O}_x$ , which resulted in the enhanced  $\text{NH}_3$ -SCR activity.

It was believed that the redox ability and adsorption of  $\text{NH}_3$  and  $\text{NO}_x$  of the catalysts played important roles in the  $\text{NH}_3$ -SCR reaction. In the present study, the  $\text{CeNb}_{3.0}\text{Zr}_2\text{O}_x$  catalyst exhibited higher redox ability than the  $\text{CeZr}_2\text{O}_x$ , indicating that the  $\text{CeNb}_{3.0}\text{Zr}_2\text{O}_x$

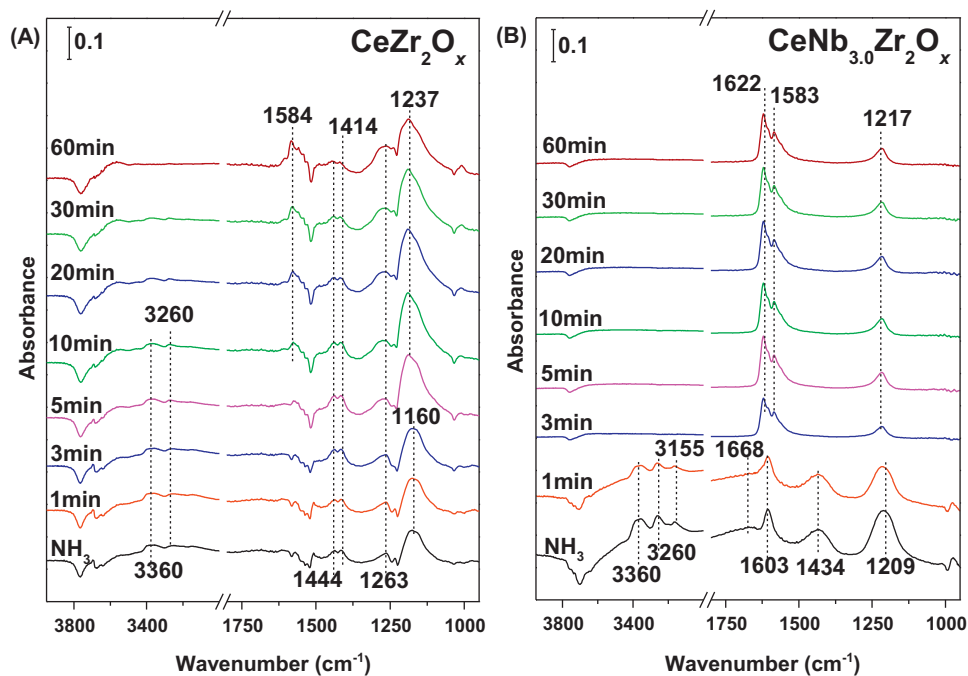


Fig. 6. *In situ* DRIFTS of NO + O<sub>2</sub> reacted with pre-adsorbed NH<sub>3</sub> species at 200 °C on CeZr<sub>2</sub>O<sub>x</sub> (A) and CeNb<sub>3.0</sub>Zr<sub>2</sub>O<sub>x</sub> (B) catalysts.

possessed high oxidation ability of NO to NO<sub>2</sub>, which was beneficial for the so-called “fast SCR”. On one hand, the addition of Nb promoted the adsorption and activation of NH<sub>3</sub>, which were considered to be a key step in the NH<sub>3</sub>-SCR process. On the other hand, the adsorption of nitrate species over CeNb<sub>3.0</sub>Zr<sub>2</sub>O<sub>x</sub> was weaker than that over CeZr<sub>2</sub>O<sub>x</sub>, due to the fact that the addition of Nb decreased the amount of basic sites where nitrate adsorbed. However, the reaction activity of adsorbed NH<sub>3</sub> and nitrate species over CeNb<sub>3.0</sub>Zr<sub>2</sub>O<sub>x</sub> was higher than that over CeZr<sub>2</sub>O<sub>x</sub>, and both of them could participate in the NH<sub>3</sub>-SCR reaction according to the *in-situ* DRIFTS results. It was likely to conclude that the adsorbed NH<sub>3</sub> species could react with adsorbed nitrate to form N<sub>2</sub> and

H<sub>2</sub>O following the Langmuir–Hinshelwood (L–H) mechanism at 200 °C.

### 3.4. Promotional effect of Nb addition on the hydrothermal stability

#### 3.4.1. Hydrothermal stability test over CeNb<sub>3.0</sub>Zr<sub>2</sub>O<sub>x</sub> and CeZr<sub>2</sub>O<sub>x</sub> catalysts

The hydrothermal stability of NH<sub>3</sub>-SCR catalysts is required in the long deNO<sub>x</sub> for practical applications, as the diesel engine exhaust temperature can reach as high as 700 °C during the regeneration process of DPF system [41]. Accordingly, the CeNb<sub>3.0</sub>Zr<sub>2</sub>O<sub>x</sub>

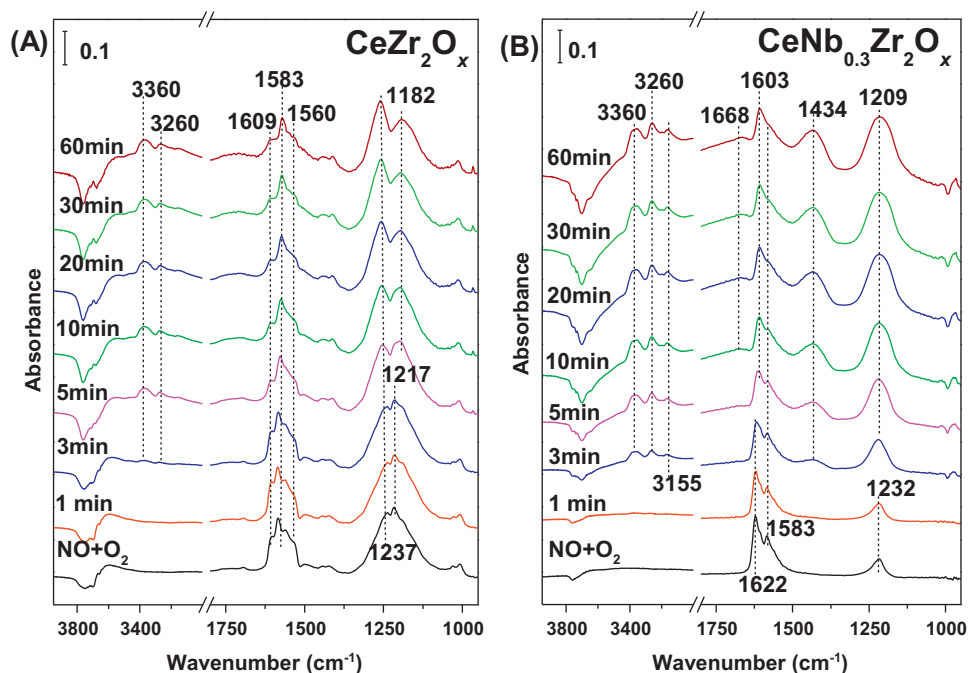
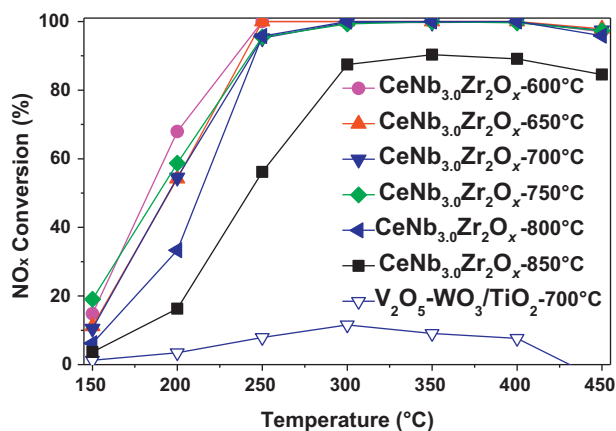
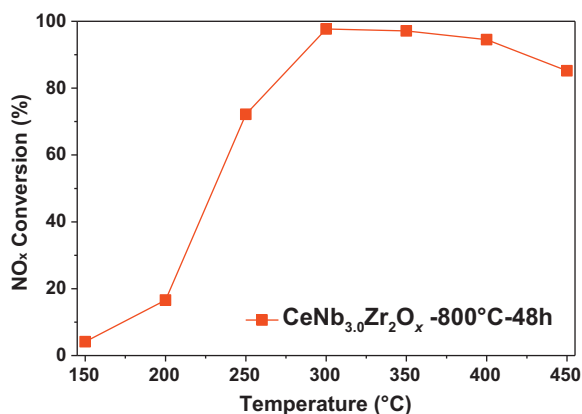


Fig. 7. *In situ* DRIFTS of NH<sub>3</sub> reacted with pre-adsorbed NO<sub>x</sub> species at 200 °C on CeZr<sub>2</sub>O<sub>x</sub> (A) and CeNb<sub>3.0</sub>Zr<sub>2</sub>O<sub>x</sub> (B) catalysts.



**Fig. 8.** NO<sub>x</sub> conversion in NH<sub>3</sub>-SCR reaction as a function of temperature over V<sub>2</sub>O<sub>5</sub>-WO<sub>3</sub>/TiO<sub>2</sub> and CeNb<sub>3.0</sub>Zr<sub>2</sub>O<sub>x</sub> catalysts aged in air containing 10 vol.% H<sub>2</sub>O at different temperatures for 8 h. Reaction conditions: [NO]=[NH<sub>3</sub>]=500 ppm, [O<sub>2</sub>]=5 vol.%, GHSV=50,000 h<sup>-1</sup>.

catalysts were hydrothermally aged at various temperatures for 8 h and the results are illustrated in Fig. 8. It was obvious that after hydrothermal treatment between 600 and 750 °C for 8 h, CeNb<sub>3.0</sub>Zr<sub>2</sub>O<sub>x</sub> catalysts showed similar SCR activity, over which more than 90% NO<sub>x</sub> conversion was obtained in the temperature range of 250–450 °C. However, further improving the hydrothermal treatment temperature to 800 and 850 °C resulted in an obvious decrease of SCR activity, which might be due to the sintering of active component. In addition, as shown in Fig. 9, CeNb<sub>3.0</sub>Zr<sub>2</sub>O<sub>x</sub> catalyst hydrothermally treated at 800 °C for 48 h still exhibited high NH<sub>3</sub>-SCR activity, over which more than 80% NO<sub>x</sub> conversion was obtained above 300 °C. For comparison purpose, the SCR activity of commercial V<sub>2</sub>O<sub>5</sub>-WO<sub>3</sub>/TiO<sub>2</sub> catalyst treated in air containing 10 vol.% H<sub>2</sub>O at 700 °C was also studied. The fresh V<sub>2</sub>O<sub>5</sub>-WO<sub>3</sub>/TiO<sub>2</sub> catalyst exhibited high activity with more than 90% NO<sub>x</sub> conversion from 250 to 450 °C (see Fig. S5). Nevertheless, the NO<sub>x</sub> conversion reduced to less than 10% in the whole temperature range after hydrothermal aging at 700 °C for 8 h. Consequently, the CeNb<sub>3.0</sub>Zr<sub>2</sub>O<sub>x</sub> showed excellent hydrothermal stability compared to conventional V-based catalyst and was a promising candidate for the removal of NO<sub>x</sub> from diesel engine exhaust. The CeZr<sub>2</sub>O<sub>x</sub> catalysts were also hydrothermally aged at various temperatures to investigate the influence of Nb additive on the hydrothermal stability of Nb containing catalysts. As shown in Fig. S6, as the calcination temperature increased from 600 to 850 °C, the NO<sub>x</sub>



**Fig. 9.** NO<sub>x</sub> conversion in NH<sub>3</sub>-SCR reaction as a function of temperature over CeNb<sub>3.0</sub>Zr<sub>2</sub>O<sub>x</sub> catalysts aged in air containing 10 vol.% H<sub>2</sub>O at 800 °C for 48 h. Reaction conditions: [NO]=[NH<sub>3</sub>]=500 ppm, [O<sub>2</sub>]=5 vol.%, GHSV=50,000 h<sup>-1</sup>.

**Table 2**

BET surface area, pore volume and H<sub>2</sub> consumption of CeNb<sub>3.0</sub>Zr<sub>2</sub>O<sub>x</sub> samples hydrothermally aged at various temperatures for 8 h

Catalysts	S <sub>BET</sub> <sup>a</sup> (m <sup>2</sup> /g)	Pore volume <sup>b</sup> (cm <sup>3</sup> /g)	H <sub>2</sub> consumption (μmol H <sub>2</sub> /g <sub>cat</sub> )
CeNb <sub>3.0</sub> Zr <sub>2</sub> O <sub>x</sub> -600 °C	136.7	0.22	469.3
CeNb <sub>3.0</sub> Zr <sub>2</sub> O <sub>x</sub> -650 °C	123.5	0.22	464.2
CeNb <sub>3.0</sub> Zr <sub>2</sub> O <sub>x</sub> -700 °C	83.5	0.11	109.7
CeNb <sub>3.0</sub> Zr <sub>2</sub> O <sub>x</sub> -750 °C	85.7	0.09	93.3
CeNb <sub>3.0</sub> Zr <sub>2</sub> O <sub>x</sub> -800 °C	85.0	0.15	73.9
CeNb <sub>3.0</sub> Zr <sub>2</sub> O <sub>x</sub> -850 °C	88.5	0.13	-

<sup>a</sup> BET surface area. <sup>b</sup>Total pore volume

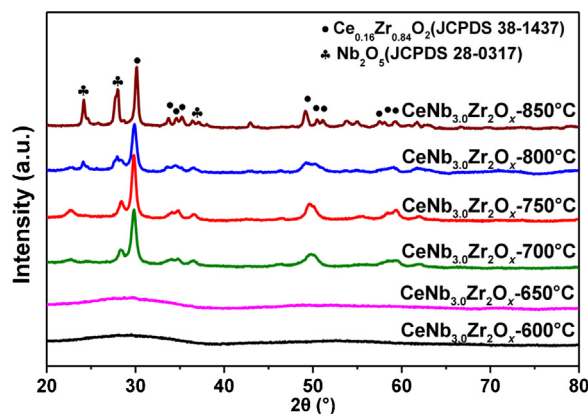


**Fig. 10.** Powder XRD results of CeNb<sub>3.0</sub>Zr<sub>2</sub>O<sub>x</sub> catalysts hydrothermally aged at different temperatures for 8 h.

conversion showed a monotonic decline in the entire temperature range. In combination with the results from Fig. 8 and S6, it was likely to conclude that the introduction of Nb to CeZr<sub>2</sub>O<sub>x</sub> significantly improved the hydrothermal stability of CeNb<sub>3.0</sub>Zr<sub>2</sub>O<sub>x</sub>. The reasons which were responsible for the high hydrothermal stability of CeNb<sub>3.0</sub>Zr<sub>2</sub>O<sub>x</sub> catalyst will be discussed later in this work.

#### 3.4.2. N<sub>2</sub> physisorption

As shown in Fig. S7, the closure point of the hysteresis loops of the samples moved to higher P/P<sub>0</sub> with the increase of hydrothermal aging temperature, indicating that more abundant macropores were formed after hydrothermal aging. Besides, the surface area and pore volume of CeNb<sub>3.0</sub>Zr<sub>2</sub>O<sub>x</sub> catalysts hydrothermally treated at different temperatures for 8 h are illustrated in Table 2. It was obvious that increasing the temperature from 600 to 700 °C gave rise to a decline of surface area from 136.7 to 83.5 m<sup>2</sup>/g. Nevertheless, the catalysts treated at 700–850 °C exhibited similar surface area about 85 m<sup>2</sup>/g, which indicated that the reduce of surface area resulting from high temperature sintering had reached to the limit above 700 °C, and surface area might not be the main factor that was responsible for the differences of NO<sub>x</sub> conversion.

#### 3.4.3. XRD results

In addition, the crystal structure of CeNb<sub>3.0</sub>Zr<sub>2</sub>O<sub>x</sub> catalysts after hydrothermal aging was also investigated. As shown in Fig. 10, the CeNb<sub>3.0</sub>Zr<sub>2</sub>O<sub>x</sub> catalysts aged at 600 and 650 °C for 8 h showed similar XRD pattern, indicating that the CeNb<sub>3.0</sub>Zr<sub>2</sub>O<sub>x</sub> exhibited strong hydrothermal durability below 650 °C. Further increasing the aging temperature to 700 °C above resulted in the formation of Nb<sub>2</sub>O<sub>5</sub> and Ce<sub>0.16</sub>Zr<sub>0.84</sub>O<sub>2</sub> solid solution due to the incorporation of Zr<sup>4+</sup> with a smaller radius into the lattice of CeO<sub>2</sub> [42]. It was interesting that even after the treatment at 700, 750 and 800 °C, CeNb<sub>3.0</sub>Zr<sub>2</sub>O<sub>x</sub> catalyst still remained more than 90% NO<sub>x</sub> conver-

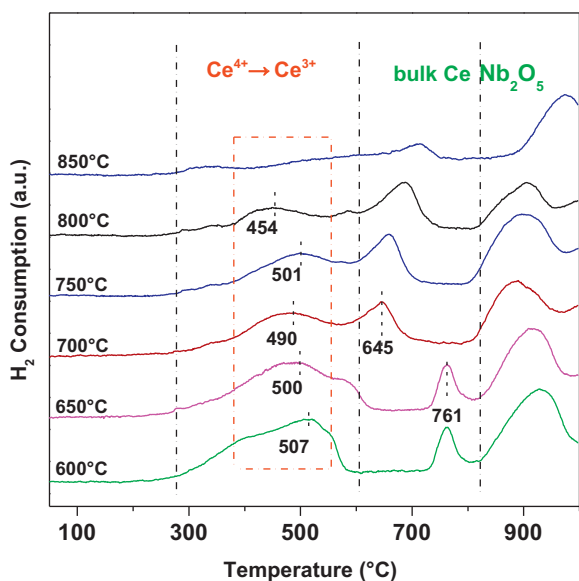


**Fig. 11.**  $H_2$ -TPR profiles of  $CeNb_{3.0}Zr_{2.0}O_x$  catalysts hydrothermally aged at various temperatures.

sion above 250 °C, which might suggest that the  $Ce_{0.16}Zr_{0.84}O_2$  solid solution was also active in  $NH_3$ -SCR reaction. Furthermore, large amount of  $Ce_{0.16}Zr_{0.84}O_2$  solid solution still existed in the  $CeNb_{3.0}Zr_{2.0}O_x$  catalyst hydrothermally treated at 850 °C. However,  $CeNb_{3.0}Zr_{2.0}O_x$ -850 °C catalyst exhibited poor SCR activity, indicating that some other factors were also essential for the activity.

#### 3.4.4. $H_2$ -TPR

The  $H_2$ -TPR results of hydrothermally aged  $CeNb_{3.0}Zr_{2.0}O_x$  catalysts are illustrated in Fig. 11. For all the catalysts, the reduction peaks less than 600 °C belonged to the reduction of surface  $Ce^{4+}$ , and the peaks centered at high temperatures were ascribed to the reduction of bulk  $CeO_2$  and  $Nb_2O_5$ . In addition, the  $H_2$  consumption for the reduction of surface  $Ce^{4+}$  to  $Ce^{3+}$  was listed in

Table 2, and it was clear that increasing the hydrothermal aging temperature from 600 to 800 °C resulted in a decrease of the  $H_2$  consumption from 469.3 to 73.9  $\mu\text{mol } H_2/\text{g}_{\text{cat}}$ . The catalysts hydrothermally aged at less than 750 °C showed similar reduction peaks centered at about 500 °C. It was likely that the similar reduction temperature was responsible for the similar  $NH_3$ -SCR activity.  $CeNb_{3.0}Zr_{2.0}O_x$ -800 °C sample showed a relative low reduction temperature around 454 °C, indicating that it should exhibit high activity. However, the lack of enough reducible surface  $Ce^{4+}$  lowered SCR conversion. For  $CeNb_{3.0}Zr_{2.0}O_x$ -850 °C sample, no obvious peak ascribed to  $Ce^{4+}$  reduction was observed, which was in highly agreement with the poor  $NO_x$  conversion. It was worth mentioning that the peaks attributed to bulk Ce showed an abrupt shift from 761 to 645 °C, as the hydrothermal treatment temperature increased from 650 to 700 °C. This may be connected with the structural change, which was proved to be true by the XRD results in Fig. 6, as the hydrothermal treatment at 700 °C led to the formation of  $Ce_{0.16}Zr_{0.84}O_2$  solid solution.

#### 3.4.5. $NH_3$ and $NO_x$ adsorption ability

In order to further investigate the influence of hydrothermal treatment on the adsorption ability of reaction species, the *in situ* DRIFTS of  $NH_3$  and  $NO_x$  adsorption at 200 °C were conducted and the results are shown in Fig. 12(A) and (B), respectively. As shown in Fig. 12(A), no obvious band ascribed to adsorbed  $NH_3$  species was observed on  $CeNb_{3.0}Zr_{2.0}O_x$  catalyst hydrothermally aged at 850 °C. However,  $CeNb_{3.0}Zr_{2.0}O_x$ -800 °C sample still possessed large amount of adsorbed  $NH_3$  species. The total amount of adsorbed  $NH_3$  species over  $CeNb_{3.0}Zr_{2.0}O_x$ -650 °C,  $CeNb_{3.0}Zr_{2.0}O_x$ -700 °C and  $CeNb_{3.0}Zr_{2.0}O_x$ -750 °C was similar. As mentioned before, acid sites played a significant role in the adsorption and activation of  $NH_3$  during the SCR process. Therefore, in combination with the  $H_2$ -TPR results of hydrothermal aged  $CeNb_{3.0}Zr_{2.0}O_x$  samples in Fig. 11, it was reasonable that the  $CeNb_{3.0}Zr_{2.0}O_x$  catalysts hydrothermally aged between 650 and 750 °C showed similar SCR activity. In addition, the amount of adsorbed  $NO_3^-$  presented a minor decline with increasing aging temperature indicating that the basic sites over  $CeNb_{3.0}Zr_{2.0}O_x$  were diminished after hydrothermal aging.

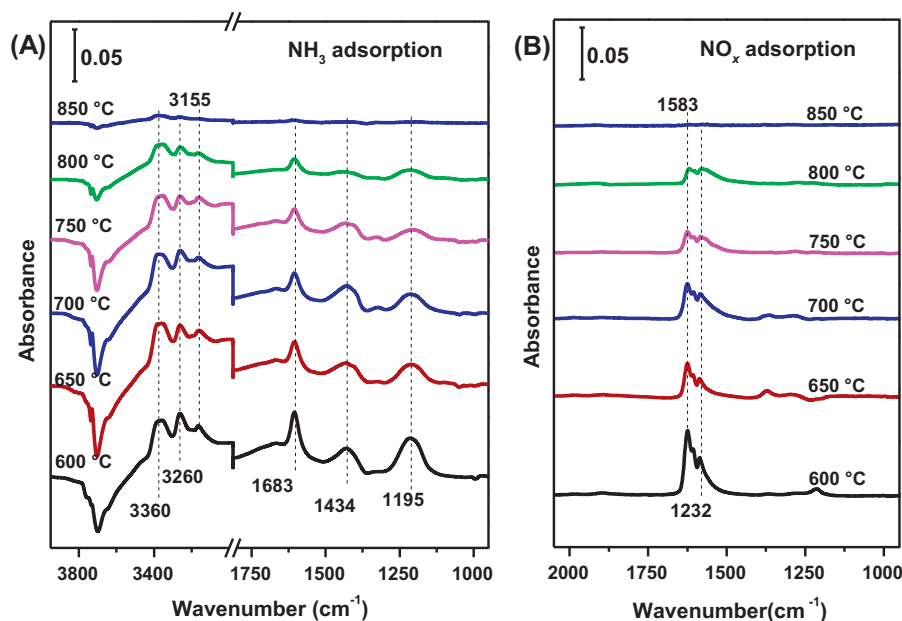


**Fig. 12.** *In situ* DRIFTS of 500 ppm  $NH_3$  adsorption (A) and 500 ppm  $NO + 5 \text{ vol.}\% O_2$  adsorption (B) with 300 mL/min flow rate at 200 °C on  $CeNb_{3.0}Zr_{2.0}O_x$  catalysts hydrothermally treated at various temperatures.

#### 4. Conclusions

A novel Nb doped CeZr<sub>2</sub>O<sub>x</sub> catalyst prepared by a homogeneous precipitation was used in the NH<sub>3</sub>-SCR reaction. CeNb<sub>3.0</sub>Zr<sub>2.0</sub>O<sub>x</sub> catalyst with the Nb/Ce molar ratio of 3.0:1 showed excellent SCR activity along with high N<sub>2</sub> selectivity, SO<sub>2</sub>/H<sub>2</sub>O resistance and remarkable hydrothermal stability. The characterization results demonstrated that the CeNb<sub>3.0</sub>Zr<sub>2.0</sub>O<sub>x</sub> catalyst, a promising NH<sub>3</sub>-SCR catalyst, possessed large surface area, strong redox ability and high reactive nitrate together with NH<sub>3</sub> species, all of which were responsible for the remarkable SCR performance. Furthermore, the CeNb<sub>3.0</sub>Zr<sub>2.0</sub>O<sub>x</sub> catalyst still remained high redox ability together with affluent acid sites after hydrothermal aging below 800 °C, and was a promising candidate for the elimination of NO<sub>x</sub> from diesel engine exhaust.

#### Acknowledgements

This work was supported by the National Natural Science Foundation of China (51221892) and the Ministry of Science and Technology, China (2013AA065301).

#### Appendix A. Supplementary data

Supplementary data associated with this article can be found, in the online version, at <http://dx.doi.org/10.1016/j.apcatb.2015.06.055>

#### References

- [1] H. Bosch, F. Janssen, Formation and control of nitrogen oxides, *Catal. Today* 2 (1988) 369–379.
- [2] G. Busca, L. Lietti, G. Ramis, F. Berti, Chemical and mechanistic aspects of the selective catalytic reduction of NO<sub>x</sub> by ammonia over oxide catalysts: a review, *Appl. Catal. B: Environ.* 18 (1998) 1–36.
- [3] V.I. Pavulescu, P. Grange, B. Delmon, Catalytic removal of NO, *Catal. Today* 46 (1998) 233–316.
- [4] F.D. Liu, H. He, Y. Ding, C.B. Zhang, Effect of manganese substitution on the structure and activity of iron titanate catalyst for the selective catalytic reduction of NO with NH<sub>3</sub>, *Appl. Catal. B: Environ.* 93 (2009) 194–204.
- [5] J.P. Dunn, P.R. Koppula, H.G. Stenger, I.E. Wachs, Oxidation of sulfur dioxide to sulfur trioxide over supported vanadia catalysts, *Appl. Catal. B: Environ.* 19 (1998) 103–117.
- [6] J. Kašpar, P. Fornasiero, M. Graziani, Use of CeO<sub>2</sub>-based oxides in the three-way catalysis, *Catal. Today* 50 (1999) 285–298.
- [7] H.W. Jen, G.W. Graham, W. Chun, R.W. McCabe, J.P. Cuif, S.E. Deutsch, O. Touret, Characterization of model automotive exhaust catalysts: Pd on ceria and ceria–zirconia supports, *Catal. Today* 50 (1999) 309–328.
- [8] M. Haneda, T. Morita, Y. Nagao, Y. Kintaichi, H. Hamada, CeO<sub>2</sub>–ZrO<sub>2</sub> binary oxides for NO<sub>x</sub> removal by sorption, *Phys. Chem. Chem. Phys.* 3 (2001) 4696–4700.
- [9] Y. Li, H. Cheng, D. Li, Y. Qin, Y. Xie, S. Wang, WO<sub>3</sub>/CeO<sub>2</sub>–ZrO<sub>2</sub>, a promising catalyst for selective catalytic reduction (SCR) of NO<sub>x</sub> with NH<sub>3</sub> in diesel exhaust, *Chem. Commun.* 12 (2008) 1470–1472.
- [10] S. Gao, X. Chen, H. Wang, J. Mo, Z. Wu, Y. Liu, X. Weng, Ceria supported on sulfated zirconia as a superacid catalyst for selective catalytic reduction of NO with NH<sub>3</sub>, *J. Colloid Interface Sci.* 394 (2013) 515–521.
- [11] Z.C. Si, D. Weng, X.D. Wu, R. Ran, Z.R. Ma, NH<sub>3</sub>-SCR activity, hydrothermal stability sulfur resistance and regeneration of Ce<sub>0.75</sub>Zr<sub>0.25</sub>O<sub>2</sub>–PO<sub>4</sub><sup>3-</sup> catalyst, *Catal. Commun.* 17 (2012) 146–149.
- [12] R.H. Gao, D.S. Zhang, P. Maitarad, L.Y. Shi, T. Rungrotmongkol, H.R. Li, J.P. Zhang, W.G. Cao, Morphology-dependent properties of MnO<sub>x</sub>/ZrO<sub>2</sub>–CeO<sub>2</sub> nanostructures for the selective catalytic reduction of NO with NH<sub>3</sub>, *J. Phys. Chem. C* 117 (2013) 10502–10511.
- [13] P. Maitarad, D.S. Zhang, R.H. Gao, L.Y. Shi, H.R. Li, L. Huang, T. Rungrotmongkol, J.P. Zhang, Combination of experimental and theoretical investigations of MnO<sub>x</sub>/Ce<sub>0.9</sub>Zr<sub>0.1</sub>O<sub>2</sub> nanorods for selective catalytic reduction of NO with ammonia, *J. Phys. Chem. C* 117 (2013) 9999–10006.
- [14] Z. Lian, F. Liu, H. He, X. Shi, J. Mo, Z. Wu, Manganese–niobium mixed oxide catalyst for the selective catalytic reduction of NO<sub>x</sub> with NH<sub>3</sub> at low temperatures, *Chem. Eng. J.* 250 (2014) 390–398.
- [15] M. Casapu, O. Krocher, M. Mehring, M. Nachttegaal, C. Borca, M. Harfouche, D. Grolimund, Characterization of Nb-containing MnO<sub>x</sub>–CeO<sub>2</sub> catalyst for low-temperature selective catalytic reduction of NO with NH<sub>3</sub>, *J. Phys. Chem. C* 114 (2010) 9791–9801.
- [16] R. Qu, X. Gao, K. Cen, J. Li, Relationship between structure and performance of a novel cerium–niobium binary oxide catalyst for selective catalytic reduction of NO with NH<sub>3</sub>, *Appl. Catal. B: Environ.* 142 (2013) 290–297.
- [17] K.S.W. Sing, D.H. Everett, R.A.W. Haul, L. Moscou, R.A. Pierotti, J. Rouquerol, T. Siemieniowska, Reporting physisorption data for gas solid systems with special reference to the determination of surface-area and porosity (recommendations 1984), *Pure Appl. Chem.* 57 (1985) 603–619.
- [18] S. Gao, P. Wang, X. Chen, H. Wang, Z. Wu, Y. Liu, X. Weng, Enhanced alkali resistance of CeO<sub>2</sub>/SO<sub>4</sub><sup>2-</sup>–ZrO<sub>2</sub> catalyst in selective catalytic reduction of NO<sub>x</sub> by ammonia, *Catal. Commun.* 43 (2014) 223–226.
- [19] P. Li, Y. Xin, Q. Li, Z.P. Wang, Z.L. Zhang, L.R. Zheng, Ce–Ti amorphous oxides for selective catalytic reduction of NO with NH<sub>3</sub>: confirmation of Ce–O–Ti active sites, *Environ. Sci. Technol.* 46 (2012) 9600–9605.
- [20] Z. Liu, J. Zhu, J. Li, L. Ma, S.I. Woo, Novel Mn–Ce–Ti mixed-oxide catalyst for the selective catalytic reduction of NO<sub>x</sub> with NH<sub>3</sub>, *ACS Appl. Mater. Interfaces* 6 (2014) 14500–14508.
- [21] X. Li, Y. Li, Selective catalytic reduction of NO with NH<sub>3</sub> over CeMoO<sub>x</sub> catalyst, *Catal. Lett.* 144 (2013) 165–171.
- [22] Y. Peng, J. Li, L. Chen, J. Chen, J. Han, H. Zhang, W. Han, Alkali metal poisoning of a CeO<sub>2</sub>–WO<sub>3</sub> catalyst used in the selective catalytic reduction of NO<sub>x</sub> with NH<sub>3</sub>: an experimental and theoretical study, *Environ. Sci. Technol.* 46 (2012) 2864–2869.
- [23] Z. Lian, F. Liu, H. He, Effect of preparation methods on the activity of VO<sub>x</sub>/CeO<sub>2</sub> catalysts for the selective catalytic reduction of NO<sub>x</sub> with NH<sub>3</sub>, *Catal. Sci. Technol.* 5 (2014) 389–396.
- [24] I.E. Wachs, L.E. Briand, J.-M. Jehng, L. Burcham, X. Gao, Molecular structure and reactivity of the group V metal oxides, *Catal. Today* 57 (2000) 323–330.
- [25] H. Xu, Y. Wang, Y. Cao, Z. Fang, T. Lin, M. Gong, Y. Chen, Catalytic performance of acidic zirconium-based composite oxides monolithic catalyst on selective catalytic reduction of NO<sub>x</sub> with NH<sub>3</sub>, *Chem. Eng. J.* 240 (2014) 62–73.
- [26] S. Cai, D. Zhang, L. Zhang, L. Huang, H. Li, R. Gao, L. Shi, J. Zhang, Comparative study of 3D ordered macroporous Ce<sub>0.75</sub>Zr<sub>0.2</sub>M<sub>0.05</sub>O<sub>2-δ</sub> (M = Fe, Cu, Mn, Co) for selective catalytic reduction of NO with NH<sub>3</sub>, *Catal. Sci. Technol.* 4 (2014) 93–101.
- [27] J. Yu, Z.C. Si, L. Chen, X.D. Wu, D. Weng, Selective catalytic reduction of NO<sub>x</sub> by ammonia over phosphate-containing Ce<sub>0.75</sub>Zr<sub>0.25</sub>O<sub>2</sub> solids, *Appl. Catal. B: Environ.* 163 (2015) 223–232.
- [28] S.Y. Christou, M.C. Alvarez-Galvan, J.L.G. Fierro, A.M. Efstathiou, Suppression of the oxygen storage and release kinetics in Ce<sub>0.5</sub>Zr<sub>0.5</sub>O<sub>2</sub> induced by P, Ca and Zn chemical poisoning, *Appl. Catal. B: Environ.* 106 (2011) 103–113.
- [29] B.Q. Jiang, Z.G. Li, S.C. Lee, Mechanism study of the promotional effect of O<sub>2</sub> on low-temperature SCR reaction on Fe–Mn/TiO<sub>2</sub> by DRIFT, *Chem. Eng. J.* 225 (2013) 52–58.
- [30] L. Chen, J. Li, M. Ge, DRIFT study on cerium–tungsten/titania catalyst for selective catalytic reduction of NO<sub>x</sub> with NH<sub>3</sub>, *Environ. Sci. Technol.* 44 (2010) 9590–9596.
- [31] X.L. Li, Y.H. Li, Molybdenum modified CeAlO<sub>x</sub> catalyst for the selective catalytic reduction of NO with NH<sub>3</sub>, *J. Mol. Catal. A: Chem.* 386 (2014) 69–77.
- [32] W.P. Shan, F.D. Liu, H. He, X.Y. Shi, C.B. Zhang, A superior Ce–W–Ti mixed oxide catalyst for the selective catalytic reduction of NO<sub>x</sub> with NH<sub>3</sub>, *Appl. Catal. B: Environ.* 115 (2012) 100–106.
- [33] Z.M. Liu, S.X. Zhang, J.H. Li, L.L. Ma, Promoting effect of MoO<sub>3</sub> on the NO<sub>x</sub> reduction by NH<sub>3</sub> over CeO<sub>2</sub>/TiO<sub>2</sub> catalyst studied with *in situ* DRIFTS, *Appl. Catal. B: Environ.* 144 (2014) 90–95.
- [34] Z.B. Wu, B.Q. Jiang, Y. Liu, H.Q. Wang, R.B. Jin, DRIFT study of manganese/titania-based catalysts for low-temperature selective catalytic reduction of NO with NH<sub>3</sub>, *Environ. Sci. Technol.* 41 (2007) 5812–5817.
- [35] N.Y. Topsoe, Mechanism of the selective catalytic reduction of nitric oxide by ammonia elucidated by *in situ* on-line Fourier transform infrared spectroscopy, *Science* 265 (1994) 1217–1219.
- [36] L. Chen, J.H. Li, M.F. Ge, L. Ma, H.Z. Chang, Mechanism of selective catalytic reduction of NO<sub>x</sub> with NH<sub>3</sub> over CeO<sub>2</sub>–WO<sub>3</sub> catalysts, *Chin. J. Catal.* 32 (2011) 836–841.
- [37] M. Casapu, O. Krocher, M. Mehring, M. Nachttegaal, C. Borca, M. Harfouche, D. Grolimund, Characterization of Nb-containing MnO<sub>x</sub>–CeO<sub>2</sub> catalyst for low-temperature selective catalytic reduction of NO with NH<sub>3</sub>, *J. Phys. Chem. C* 114 (2010) 9791–9801.
- [38] F.D. Liu, K. Asakura, H. He, Y.C. Liu, W.P. Shan, X.Y. Shi, C.B. Zhang, Influence of calcination temperature on iron titanate catalyst for the selective catalytic reduction of NO<sub>x</sub> with NH<sub>3</sub>, *Catal. Today* 164 (2011) 520–527.
- [39] F.D. Liu, W.P. Shan, Z.H. Lian, L.J. Xie, W.W. Yang, H. He, Novel MnWO<sub>x</sub> catalyst with remarkable performance for low temperature NH<sub>3</sub>-SCR of NO<sub>x</sub>, *Catal. Sci. Technol.* 3 (2013) 2699–2707.
- [40] B. Tsyntsarski, V. Avreyska, H. Kolev, T. Marinova, D. Klissurski, K. Hadjiivanov, FT-IR study of the nature and reactivity of surface NO<sub>x</sub> compounds formed after NO adsorption and NO + O<sub>2</sub> coadsorption on zirconia- and sulfated zirconia-supported cobalt, *J. Mol. Catal. A: Chem.* 193 (2003) 139–149.
- [41] X.Q. Wang, A.J. Shi, Y.F. Duan, J. Wang, M.Q. Shen, Catalytic performance and hydrothermal durability of CeO<sub>2</sub>–V<sub>2</sub>O<sub>5</sub>–ZrO<sub>2</sub>/WO<sub>3</sub>–TiO<sub>2</sub> based NH<sub>3</sub>-SCR catalysts, *Catal. Sci. Technol.* 2 (2012) 1386–1395.
- [42] J. Liu, Z. Zhao, C. Xu, A. Duan, L. Wang, S. Zhang, Synthesis of nanopowder Ce–Zr–Pr oxide solid solutions and their catalytic performances for soot combustion, *Catal. Commun.* 8 (2007) 220–224.